

## CRYSTALLOGRAPHY

# Coordinative alignment of molecules in chiral metal-organic frameworks

 Seungkyu Lee,<sup>1,2,3,4</sup> Eugene A. Kapustin,<sup>1,2,3,4</sup> Omar M. Yaghi<sup>1,2,3,4,5\*</sup>

A chiral metal-organic framework, MOF-520, was used to coordinatively bind and align molecules of varying size, complexity, and functionality. The reduced motional degrees of freedom obtained with this coordinative alignment method allowed the structures of molecules to be determined by single-crystal x-ray diffraction techniques. The chirality of the MOF backbone also served as a reference in the structure solution for an unambiguous assignment of the absolute configuration of bound molecules. Sixteen molecules representing four common functional groups (primary alcohol, phenol, vicinal diol, and carboxylic acid), ranging in complexity from methanol to plant hormones (gibberellins, containing eight stereocenters), were crystallized and had their precise structure determined. We distinguished single and double bonds in gibberellins, and we enantioselectively crystallized racemic jasmonic acid, whose absolute configuration had only been inferred from derivatives.

Single-crystal x-ray diffraction is a powerful technique for the definitive identification of chemical structures. Although most molecules and molecular complexes can be crystallized, often enthalpic and entropic factors introduce orientational disorder that prevents determination of a high-resolution structure (*I*). Several strategies based on the inclusion of guests in a host framework (*2–4*) that helps maintain molecular orientation have been used to overcome this challenge. However, most of these methods rely primarily on weak interactions to induce crystalline order of the included molecules.

Here, we demonstrate a strategy for crystallization of molecules within the pores of chiral metal-organic frameworks (MOFs) (*5*). This strategy provides the following advantages: (i) The molecules make covalent bonds to well-defined metal sites of the MOF; these bonds anchor them and lower their motional degrees of freedom, thereby promoting their alignment into an ordered pattern across the interior of the crystalline framework. (ii) The absolute structure of the chiral MOF serves as a reference for the direct determination of the absolute configuration of bound chiral molecules (*6*). This latter feature avoids the reported pseudosymmetry problems that have obscured the absolute structures that specify the enantiomorph in achiral host framework systems (*7–9*).

Specifically, we used this coordinative alignment (CAL) method to successfully crystallize 16 different molecules in the interior of MOF-520 [ $\text{Al}_8(\mu\text{-OH})_8(\text{HCOO})_4(\text{-COO})_{12}$  (BTB)<sub>4</sub>; BTB = 1,3,5-benzenetribenzoate] (*10*). These molecules represent a range of functionality, flexibility, and complexity. The first 12 are relatively simple molecules: benzoic acid **1**, methanol **2**, ethylene glycol **3**, 3-nitrophenol **4**, heptanoic acid **5**, 3-hydroxybenzoic acid **6**, 3,5-diaminobenzoic

acid **7**, trimesic acid **8**, 4-bromophenol **9**, 2-(2,6-dichloranilino)phenylacetic acid (diclofenac) **10**, 5,7-dihydroxy-3-(4-hydroxyphenyl)chromen-4-one (genistein) **11**, and *tert*-butyloxycarbonyl-(*RS*)-3-amino-1,2-propanediol **12**. In addition, this method led us to successfully crystallize two different

plant hormone types within the MOF: gibberellins (form A<sub>1</sub>, **13**, and form A<sub>3</sub>, **14**) with eight stereocenters, and (±)-jasmonic acid (**15**, **16**). The precision of the crystal structures with only 30% occupancy of the bound gibberellins enabled us to distinguish the single bond in **13** from the double bond in **14**, this being the only difference between the two complex molecules. The crystal structure of (±)-jasmonic acid, whose absolute configuration had only been inferred from derivatives, was obtained enantioselectively, with each enantiomorph of the MOF binding only one enantiomer of jasmonic acid.

We chose MOF-520 as the framework for implementing the CAL method of crystallization because of its high crystallinity, robustness, and chirality (Fig. 1). Its secondary building units (SBUs) are rings of eight aluminum octahedra sharing corners through eight μ-OHs and four formate ligands. Each of these SBUs is linked by 12 BTB units, and each BTB is linked to three SBUs to make a three-dimensional, extended porous framework. Two types of ellipsoidal pores are formed from elongated arrangements of SBUs that are octahedral (10.01 Å × 10.01 Å × 23.23 Å) and tetrahedral (5.89 Å × 5.89 Å × 6.21 Å). The framework of MOF-520 crystallizes in the noncentrosymmetric space group *P*4<sub>2</sub>2<sub>1</sub>2, with a chiral atomic arrangement. The absolute

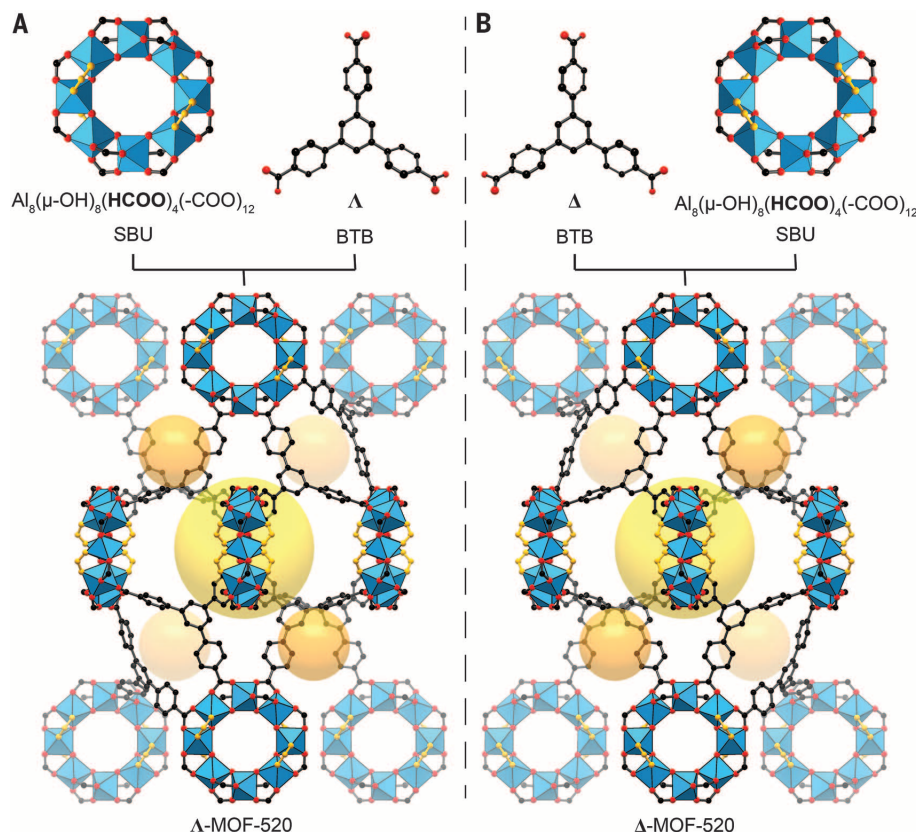


**Fig. 1. Structures of MOF-520 enantiomorphs and their building units.** MOF-520 comprises the SBU,  $\text{Al}_8(\mu\text{-OH})_8(\text{HCOO})_4(\text{-COO})_{12}$ , and BTB linker. Each SBU is coordinated by 16 carboxylates, 12 from BTB linkers and 4 from formate ligands (highlighted in yellow on the SBU). The absolute structure descriptors  $\Delta$ -MOF-520 (**A**) and  $\Lambda$ -MOF-520 (**B**) are assigned on the basis of absolute configuration of the BTB linker. The large yellow and small orange balls represent the octahedral and tetrahedral pores, respectively. Color code: black, C; red, O; blue polyhedra, Al.

<sup>1</sup>Department of Chemistry, University of California, Berkeley, CA 94720, USA. <sup>2</sup>Materials Sciences Division, Lawrence Berkeley National Laboratory, Berkeley, CA 94720, USA. <sup>3</sup>Kavli Energy NanoSciences Institute, Berkeley, CA 94720, USA. <sup>4</sup>Berkeley Global Science Institute, Berkeley, CA 94720, USA. <sup>5</sup>King Abdulaziz City for Science and Technology, Riyadh 11442, Saudi Arabia. \*Corresponding author. Email: yaghi@berkeley.edu

structure of each enantiomorph is designated as  $\Lambda$  or  $\Delta$  according to the chirality of the BTB linker in the respective crystal structure (Fig. 1, A and B). Although each single crystal is nearly enantiomorphically pure according to the Flack parameters of the refined structures—0.049(17) for  $\Lambda$  and 0.031(11) for  $\Delta$  (11)—the overall bulk sample is a racemic conglomerate containing both enantiomorphs (tables S1 to S3).

The distinctive nature of this MOF lies in each of the aluminum SBUs having four formate ligands in addition to 12 carboxyl units from BTB linkers to complete the octahedral coordination sites of the aluminum centers (Fig. 1). These formate ligands occupy two sites on each face of the SBU in a chiral tetrahedral arrangement with  $D_2$  symmetry. We anticipated that through acid-base chemistry, we could substitute these formates with incoming organic molecules such as carboxylates, alkoxides, and phenolates (Fig. 2A). Given that the interior of the MOF has large octahedral pores, it is reasonable to expect molecules of varying size and complexity to diffuse into this space and covalently bind to the metal sites (Fig. 2B), thereby aligning themselves within the MOF to be amenable to x-ray structure determination (see below).

Before examining the incorporation of molecules into the pores of MOF-520, we used single-crystal x-ray diffraction (SXRD) techniques (10, 12) to ensure full characterization of the structure of the MOF. We confirmed the chemical composition of the evacuated MOF-520 by  $^1\text{H}$  nuclear magnetic resonance (NMR) of digested samples (calculated formate/BTB ratio, 1:1; found, 1:0.93) and by elemental analysis [calculated weight percent (wt %), C 58.81, H 3.14, N 0.0; found wt %, C 59.20, H 3.19, N < 0.2]. The porosity of MOF-520 was confirmed by measurement of  $\text{N}_2$  type I isotherm at 77 K, which led to a final uptake

of  $770 \text{ cm}^3 \text{ g}^{-1}$  at 1 atm, similar to a calculated uptake,  $821 \text{ cm}^3 \text{ g}^{-1}$ , based on the structure obtained from the SXRD data (both values at standard temperature and pressure). The MOF-520 samples were also characterized by infrared spectroscopy to ensure the absence of solvent in the pores, thermal gravimetric analysis to confirm the thermal stability of the MOF, and powder x-ray diffraction to confirm the bulk purity of the crystals (12).

Molecules **1** to **16** have functionalities that include primary alcohol, phenol, vicinal diol, and carboxylic acid (Fig. 2A). These molecules were covalently bonded to the MOF by immersion of single crystals of MOF-520 in a concentrated solution of the respective molecule followed by heating ( $40^\circ$  to  $100^\circ\text{C}$ ) for at least 12 hours (12). One of the single crystals in the resulting racemic conglomerate batch was chosen and SXRD data were collected. The architectural robustness and high chemical stability of MOF-520 enabled the substitution of the symmetrically equivalent four formates in the SBU with the carboxylates of incoming molecules and their covalent binding to the SBUs with full retention of crystallinity. In the case of alkoxides and phenolates, only two formates on the same face of the SBU were replaced in addition to  $\mu\text{-OHs}$  (Fig. 2B). This substitution pattern led to a doubling of the unit cell in the  $c$ -direction without affecting the connectivity of the MOF backbone. Consecutive SBUs along  $c$  were substituted strictly on the opposite face of the ring, leading to a change in the space groups of the  $\Lambda$ - and  $\Delta$ -frameworks,  $P4_32_12$  ( $\Lambda$ ) and  $P4_12_12$  ( $\Delta$ ), respectively.

Relatively small achiral molecules were chosen to describe in detail the four different binding modes in  $\Delta$ -MOF-520 for all incoming molecules: benzoic acid **1** as a carboxylic acid, methanol **2** as a primary alcohol, ethylene glycol **3** as a vicinal

diol, and 3-nitrophenol **4** as a phenol. Benzoic acid shared the same binding mode as formate, where for **2**, two methoxides replaced two formates on the same face of the ring and doubly bridged the Al in a  $\mu^2$  manner, thus changing the corner-sharing Al octahedra to edge-sharing. This geometry change induced further substitution of two  $\mu\text{-OHs}$  with the methoxides. Overall, four alkoxides replaced two formates and two  $\mu\text{-OHs}$ , with two coordinated formates remaining on the  $C_2$  symmetric SBU. The binding mode of **3** was similar to that of **2**, where the formates and  $\mu\text{-OHs}$  were substituted and the same geometry change of the SBU occurred. The main difference is that the remaining two formates are now bonded to the SBU as terminal ligands, which had previously been bridging ligands on the SBU of  $\Delta$ -MOF-520. In the case of **4**, two different binding modes were observed with positional disorder; one is similar to that of **2**, and the other is shown in Fig. 2B (two of four phenolic oxygen atoms are bridging).

The resulting substituted frameworks, MOF-520-**2** and MOF-520-**3**, have a larger pore width relative to the original MOF-520 [distance between the Al atoms of adjacent SBUs =  $14.70 \pm 0.04 \text{ \AA}$  and  $14.13 \pm 0.05 \text{ \AA}$ , respectively, versus  $13.73 \pm 0.04 \text{ \AA}$  for MOF-520] (fig. S16). Thus, we used MOF-520 for the crystallization of incoming molecules **1** to **10**, **12**, **15**, and **16**; MOF-520-**2** for **11**; and MOF-520-**3** for **13** and **14**.

The crystal structures of all molecules bound to the MOF were determined by SXRD and show the binding modes outlined above. All of the structures were refined anisotropically (Fig. 3). In general, the value of anisotropic displacement parameters of the incorporated molecules increased with their distance from the binding sites; this was as expected, because the orientations of the bound

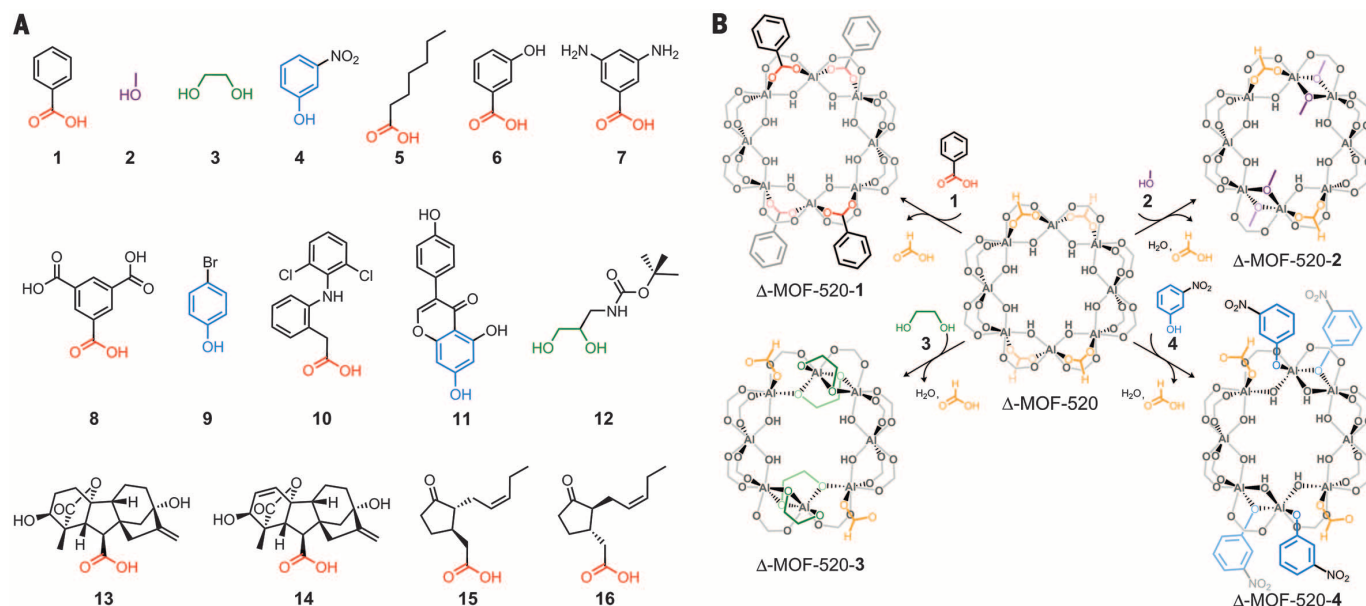


**Fig. 2. Structures of incoming molecules (1 to 16) and coordination modes of their deprotonated forms on the SBU of  $\Delta$ -MOF-520.** (A) The structures of **1** to **16** represent the molecules binding to the SBU, where their functionalities are highlighted with colors: red, carboxylic acid; purple, primary alcohol; green, vicinal diol; blue, phenol. (B) The SBU of  $\Delta$ -MOF-520 is shown in the center, with the four formate ligands (yellow) highlighted. The deprotonated forms of **1** to **4** replace all (**1**) or some (**2** to **4**) of the formate ligands and  $\mu\text{-OH}$  on the SBU; the resulting coordination modes and the functionalities of the molecules are colored. For clarity, the chiralities of  $\Lambda$ -MOF-520-**2** and -**4** are converted to  $\Delta$  configuration.

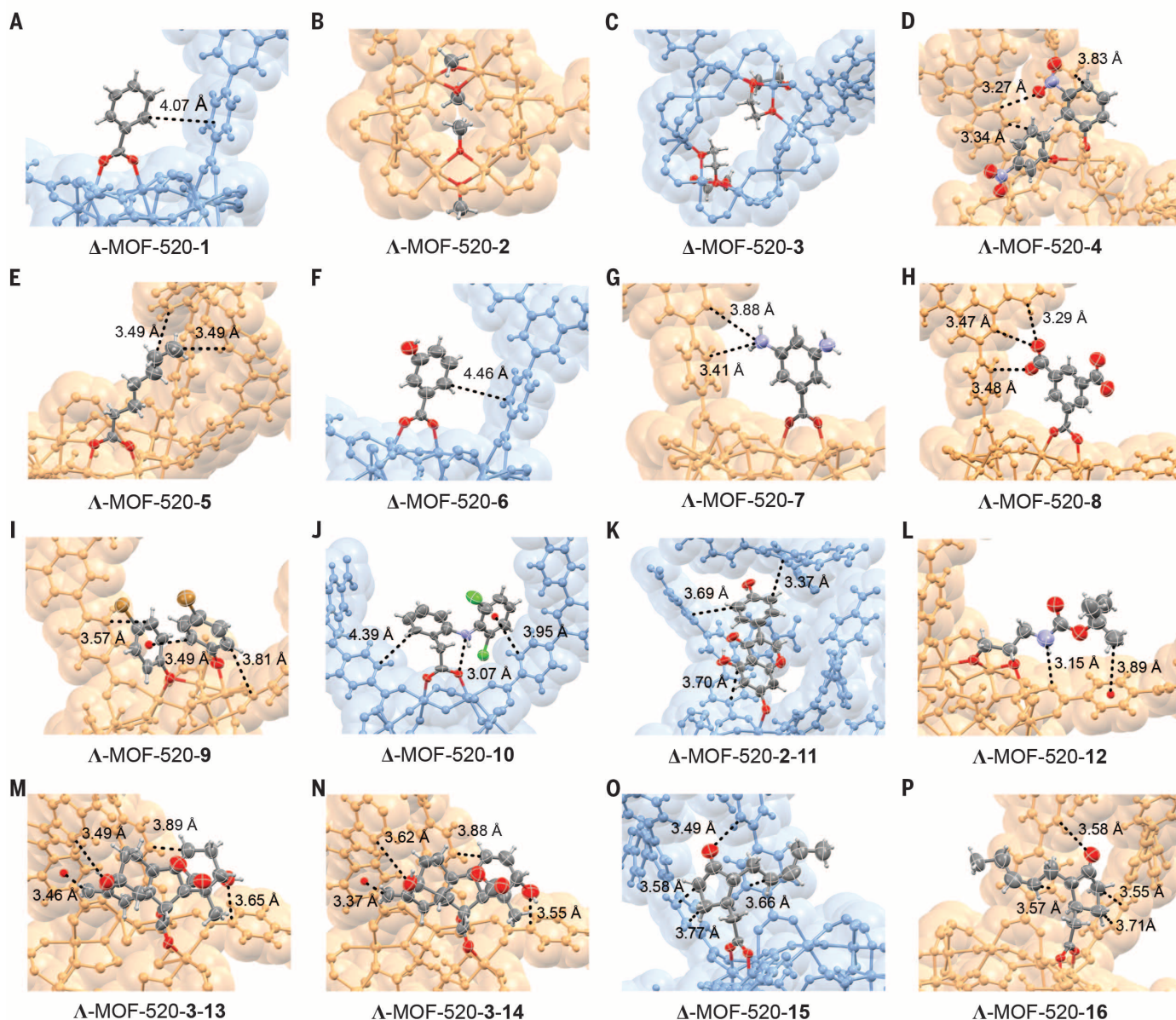


**Fig. 3. Refined structures of 1 to 16 crystallized in  $\Lambda$ - or  $\Delta$ -MOF-520.** (A to P) The refined structures of the molecules obtained from SXRD data are indicated with 50% probability thermal ellipsoids. The surroundings of the coordination sites of  $\Lambda$ - and  $\Delta$ -MOF-520 are shown with orange and blue space-filling models, respectively. Intramolecular interactions [except for (A) and (F)] between the moieties of the molecules and the surroundings of the coordination sites are indicated with dotted lines and distances (Å). In the case of positional disorder, only one conformation of bound molecules is shown for clarity. Color code: gray, C; red, O; white, H; pale violet, N; green, Cl; brown, Br.

molecules are mainly governed by a single site of covalent attachment. Those parts of the bound molecules that are far from the binding sites are stabilized by noncovalent interactions such as  $\pi$ - $\pi$  interactions and weak hydrogen bonds with the aromatic rings and carboxylates of the framework (Fig. 3 and table S4).

The bound molecules **1**, **2**, **3**, and **6** are simple and small in their structure; their ordering within the MOF is sustained only by covalent bonds to aluminum, with no weak interactions with the framework observed (Fig. 3, A, B, C, and F). The covalent binding is sufficient to anchor these molecules and lower their degrees of freedom, an aspect that

is present in all crystal structures of **1** to **16**; weak interactions play a role for some molecules but not all. For example, in  $\Delta$ -MOF-520-**6**, the closest distance from the covalent bond **6** to the framework is 4.46 Å, which corresponds to the distance between the *ortho*-carbon of **6** and the adjacent aromatic ring of the MOF; this indicates that there are no contributing secondary interactions with the framework (Fig. 3F). However, the entire structure of **6** was solved without ambiguity. The OH group of **6** is pointing away from the framework, which suggests a possible repulsive interaction with the adjacent aromatic ring of the linker. No detectable residual electron density was observed in

the structure refinement for the second OH group at the other *meta* position.

Within the MOF, molecules **10** and **11** were also ordered by anchoring through covalent bonding to aluminum, but their order was further enhanced by the presence of  $\pi$ - $\pi$  (T-shaped for **10** and parallel-displaced for **11**) and hydrogen bonding (N-H $\cdots$ O for **10** and O-H $\cdots$  $\pi$  for **11**) interactions to the framework (Fig. 3, J and K). Similar interactions were also observed for the molecules **4**, **5**, **7** to **9**, and **12** to **16**. Details of the structural information (including the covalent bond distances, the types of closest noncovalent interactions between the bound molecules and

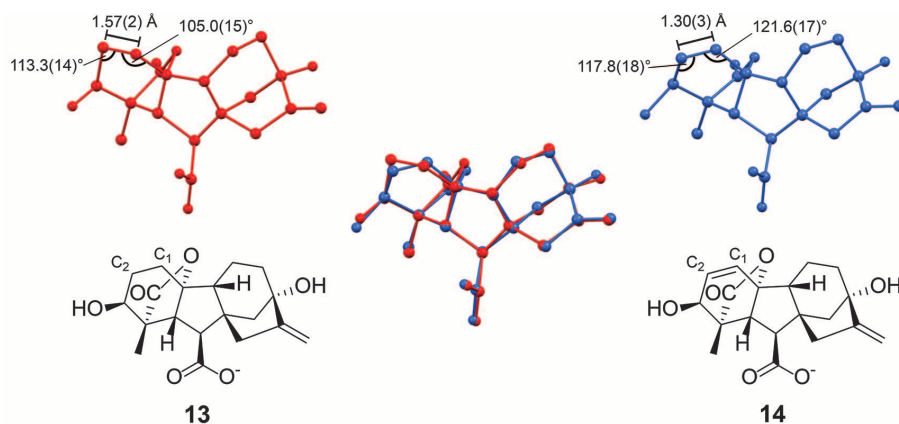


**Fig. 4. Comparison of the molecular geometries of **13** and **14**.** Ball-and-stick models of the structures of **13** and **14** crystallized in  $\Delta$ -MOF-520-**3** are shown in red and blue, respectively. Their conformations are overlaid in the middle. The structural difference, a single bond between C<sub>1</sub> and C<sub>2</sub> for **13** and a double bond for **14**, can be distinguished from the distances and the angles indicated on the models. For clarity, only atoms C<sub>1</sub> and C<sub>2</sub> are labeled.

the framework, and refinement parameters) are given in table S4.

Because the CAL method yields highly ordered arrangements for molecules within the MOF, their structure can be determined even with low occupancy at the binding sites. This feature makes it possible to obtain structures of larger and more complex molecules with high accuracy and to determine the absolute configuration of chiral molecules with high certainty. The structures of gibberellins **13** and **14**, two derivatives of a natural plant hormone, illustrate the power of the CAL method (Fig. 3, M and N, and Fig. 4). All non-hydrogen atoms of these complex molecules with eight stereocenters could be assigned from an occupancy of only 30%. The final structures were refined without any geometrical constraints or restraints applied on the gibberellin molecules (tables S17 and S18). The accuracy of our method is documented by the characterization of the subtle structure difference between **13** and **14**, where we find C<sub>1</sub>-C<sub>2</sub> to be a single bond ( $1.57 \pm 0.02$  Å) in **13** and a double bond ( $1.30 \pm 0.03$  Å) in **14**. The C-C bond angles at C<sub>1</sub> and C<sub>2</sub> are  $105.0^\circ \pm 1.5^\circ$  and  $113.3^\circ \pm 1.4^\circ$  in **13** and  $121.6^\circ \pm 1.7^\circ$  and  $117.8^\circ \pm 1.8^\circ$  in **14**, indicative of sp<sup>3</sup> and sp<sup>2</sup> hybridization, respectively. Ball-and-stick representations of the structures are superimposed for direct comparison in Fig. 4.

The absolute structures of  $\Delta$ -MOF-520-**3**-**13** and -**14** were assigned on the basis of their Flack parameters—0.063(9) and 0.05(2), respectively—despite the low occupancies of the molecules. In previous reports, the absolute configurations of the guests were determined in achiral host frameworks (7–9, 13). In those methods, pseudocentrosymmetry problems were reported and the absolute structure determinations were obscured, even though the structures of the guests were identified in the structure solution. This problem may be caused by several factors, such as low guest occupancy (7, 9), lack of high-angle reflections because of disorder of the guest (9, 14), and the nearly centrosymmetric nature of the guest (8, 9, 15). The chiral MOFs show anomalous scattering from the framework itself,

regardless of any included chiral molecules (15, 16). The strong enantiomorph-distinguishing power originates mainly from the scattering of the chiral framework and is enhanced by chiral and achiral bound molecules. It is sufficient for determining the absolute structure of the resulting crystal, including the absolute configuration of the bound molecule, even when the occupancy of the latter is low.

One advantage of the CAL method for the determination of the absolute configuration of molecules is that it may reduce dependence on the absolute structure parameters of the inclusion crystal data. For example, when a single crystal with absolute structure  $\Lambda$  has been determined by SXRD and subsequently used in the inclusion, the absolute configuration of the incorporated molecule can be directly deduced from the predetermined  $\Lambda$  structure. In this case, the correctness of the absolute configuration of incorporated molecules is highly dependent on the predetermined absolute structure and the knowledge of the enantiopurity of the single crystal used for the inclusion (6).

Finally, to demonstrate that the chirality of the binding sites of MOF-520 can separate enantiomers when one of them interacts more favorably with the binding site of one of the enantiomorphs of the MOF, we determined the absolute configuration of another plant hormone, jasmonic acid, for which a crystal structure has heretofore not been reported. A solution of a racemic mixture of (–)-jasmonic acid **15** and (+)-jasmonic acid **16** was reacted with a racemic conglomerate of MOF-520, and SXRD data for two enantiomorphous crystals were collected after the reaction. The molecules **15** and **16** selectively attached to  $\Delta$ -MOF-520 and  $\Lambda$ -MOF-520, respectively (Fig. 3, O and P). The positions of the last three carbons were not clearly defined, presumably because of their conformational flexibility, the low occupancy of 33%, and the ensuing overlap with the electron density of residual disordered solvent. However, the atoms defining the stereocenters of **15** and their absolute configurations, *R* for C<sub>3</sub> and *R* for C<sub>7</sub>, were observed un-

ambiguously with a Flack parameter of 0.037(8). This result corresponds to that deduced from the absolute configurations of a derivative of **15**, (–)-methyl jasmonate, which were determined by a synthetic approach (17). The enantiomer **16** attached to  $\Lambda$ -MOF-520 showed the opposite absolute configuration, as indicated by a refined Flack parameter of 0.040(8). We note that the enantiomerically pure molecules **13** and **14** had an occupancy that was sufficiently high for unambiguous structure and absolute configuration determination only in one of the two enantiomorphs. This enantioselective binding can potentially be applied to the absolute configuration determination of samples that contain a minor enantiomer, without the need for chiral high-performance liquid chromatography separation before carrying out the inclusion procedure (7).

## REFERENCES AND NOTES

1. A. Holden, P. Morrison, *Crystals and Crystal Growing* (MIT Press, 1982).
2. J. L. Atwood, J. E. D. Davies, D. D. MacNicol, *Inclusion Compounds: Structural Aspects of Inclusion Compounds Formed by Inorganic and Organometallic Host Lattices* (Academic Press, 1984).
3. Y.-M. Legrand, A. van der Lee, M. Barboiu, *Science* **329**, 299–302 (2010).
4. Y. Inokuma *et al.*, *Nature* **495**, 461–466 (2013).
5. H. Furukawa, K. E. Cordova, M. O’Keeffe, O. M. Yaghi, *Science* **341**, 1230444 (2013).
6. H. D. Flack, G. Bernardinelli, *Acta Crystallogr. A* **55**, 908–915 (1999).
7. S. Yoshioka, Y. Inokuma, M. Hoshino, T. Sato, M. Fujita, *Chem. Sci.* **6**, 3765–3768 (2015).
8. E. Sanna *et al.*, *Chem. Sci.* **6**, 5466–5472 (2015).
9. M. Hoshino, A. Khutia, H. Xing, Y. Inokuma, M. Fujita, *IUCr J* **3**, 139–151 (2016).
10. F. Gándara, H. Furukawa, S. Lee, O. M. Yaghi, *J. Am. Chem. Soc.* **136**, 5271–5274 (2014).
11. H. D. Flack, G. Bernardinelli, *J. Appl. Crystallogr.* **33**, 1143–1148 (2000).
12. See supplementary materials on Science Online.
13. T. R. Ramadhar, S.-L. Zheng, Y.-S. Chen, J. Clardy, *Acta Crystallogr. A* **71**, 46–58 (2015).
14. H. D. Flack, G. Bernardinelli, D. A. Clemente, A. Linden, A. L. Spek, *Acta Crystallogr. B* **62**, 695–701 (2006).
15. H. D. Flack, U. Shmueli, *Acta Crystallogr. A* **63**, 257–265 (2007).
16. J. M. Bijvoet, A. F. Peerdeman, A. J. van Bommel, *Nature* **168**, 271–272 (1951).
17. R. K. Hill, A. G. Edwards, *Tetrahedron* **21**, 1501–1507 (1965).

## ACKNOWLEDGMENTS

Supported by BASF SE (Ludwigshafen, Germany) for the synthesis, and by King Abdulaziz City for Science and Technology (Center of Excellence for Nanomaterials and Clean Energy Applications) for the characterization of compounds. We thank S. Teat for synchrotron x-ray diffraction data acquisition support at beamline 11.3.1 [Advanced Light Source (ALS), Lawrence Berkeley National Laboratory (LBNL)]; K. Gagnon for discussion of structure refinement; and H.-B. Bürgi for invaluable discussions of structure refinement and editing of this manuscript. NMR data were acquired at the Molecular Foundry, LBNL. Work performed at ALS and the Molecular Foundry is supported by the Office of Science, Office of Basic Energy Sciences, of the U.S. Department of Energy under contract DE-AC02-05CH11231 (ALS and Foundry). Use of CheXray facility at the College of Chemistry (UC Berkeley) is supported by NIH Shared Instrumentation grant S10-RR021712. Data reported in this paper are tabulated in the supplementary materials and archived at the Cambridge Crystallographic Data Centre under reference numbers CCDC 1488938 to 1488955.

## SUPPLEMENTARY MATERIALS

www.sciencemag.org/content/353/6301/808/suppl/DC1  
Materials and Methods  
Figs. S1 to S29  
Tables S1 to S20  
References (18–22)

19 April 2016; accepted 7 July 2016  
10.1126/science.aaf9135



## Coordinative alignment of molecules in chiral metal-organic frameworks

Seungkyu Lee, Eugene A. Kapustin and Omar M. Yaghi (August 18, 2016)

*Science* **353** (6301), 808-811. [doi: 10.1126/science.aaf9135]

Editor's Summary

### Stop wiggling and hold that pose

X-ray crystallography can be the definitive method for determining the structure and chirality of small organic molecules, but orientational disorder in the crystal can limit its resolution. Lee *et al.* used a chiral metal-organic framework containing formate ligands that can bind and align molecules covalently to reduce this motion (see the Perspective by Öhrström). The structure and absolute configuration—i.e., which spatial arrangement of atoms is the *R* or *S* isomer—of several organic molecules can thus be measured. These range from small molecules, such as methanol, to complex plant hormones, such as gibberellins that have eight stereocenters or jasmonic acid, whose absolute configuration had not previously been directly established.

*Science*, this issue p. 808; see also p. 754

---

This copy is for your personal, non-commercial use only.

---

**Article Tools** Visit the online version of this article to access the personalization and article tools:  
<http://science.sciencemag.org/content/353/6301/808>

**Permissions** Obtain information about reproducing this article:  
<http://www.sciencemag.org/about/permissions.dtl>

*Science* (print ISSN 0036-8075; online ISSN 1095-9203) is published weekly, except the last week in December, by the American Association for the Advancement of Science, 1200 New York Avenue NW, Washington, DC 20005. Copyright 2016 by the American Association for the Advancement of Science; all rights reserved. The title *Science* is a registered trademark of AAAS.